

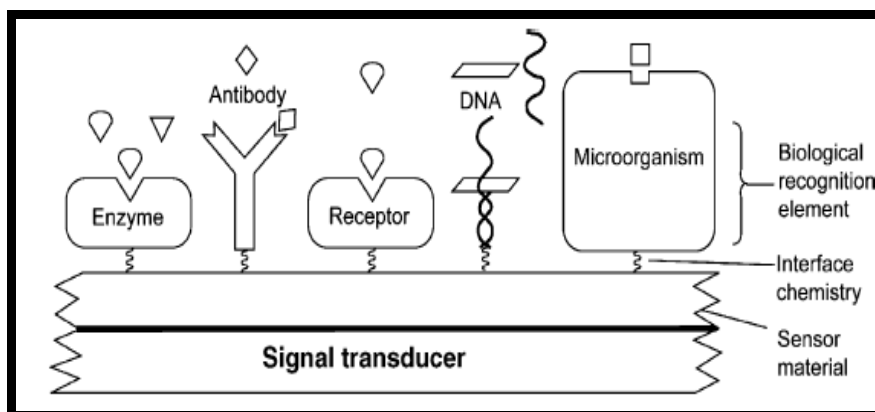
SYNTHESIS OF METAL NANOPARTICLES AND THEIR USE IN ELECTROCHEMICAL BIOSENSORS FOR THE DETECTION OF MICROBES

¹Harish Kumar, ²Bhawana

Material Science and Electrochemistry Lab., Department of Chemistry, Ch. Devi Lal
University, Sirsa- 125 055 (Haryana) (India)

ABSTRACT

One of the important applications of electrochemical biosensor is their use in the detection of microorganisms (bacteria, virus, spores, fungi, pathogens etc.) present in air, water, food, soil etc. Nanoparticles of different metals were synthesized for this purpose by the Co-precipitation method. Characterization of metal nanoparticles was carried out by XRD, FTIR, TEM and UV-Visible spectroscopic techniques. Nanoparticles based working electrode was fabricated for this purpose and then combined with two other electrodes i.e. Ag/AgCl reference and a platinum counter electrode to study its application as electrochemical biosensors in the detection of microbes present in analyte.



Keywords: Co-precipitation, Electrochemical biosensor, metal nanoparticles, Microorganisms.

I. INTRODUCTION

Nanomaterials have gained a great research interest in analytical chemistry because of their properties (e.g., size, conductivity, mechanical strength, magnetism, and light absorption and emission). The nanomaterials are being used in the environmental analysis and their use is being grown rapidly. Being present in laboratories for a long



time, they have become a great issue due to their increasing use in many consumer products and release in environment. But now, people are looking for safety concerns about nanomaterials [1-4].

Over past some years, nanomaterials, their synthesis and understanding their properties; the advancements in them have been substantial. Carbon-based nanostructures like carbon nanotubes, graphene and graphene oxide, have been collecting the attention of people in the field of material science [5]. Because of their physical, chemical and electrical properties, carbon-based nanomaterials are emerging as good materials for development of different types of biosensors [6-8]. The technology has evolved since the appearance of the first biosensor [9], but still the expected devices have not been crowned that would work as easy as other devices do. Such devices for the detection of many analytes like DNA etc. that can be low cost and more efficient are still in the way.

Using the principle of the immune chromatography, development of paper-based biosensors seems to be the possible path that can take this research to its future- says (IAs) [10-14]. The separation of analytes which flow across a porous medium taking into account the specific interactions that occur between antigen and antibody, enzyme and substrate, or receptor and ligand. Paper is easy to manufacture which is cheap and simple too and it also fulfills all the requirements related to cost and efficiency in biosensing technology [15].

Bioterrorism is the use of a biological weapon (bacteria, virus or spores) on human life as a weapon of mass infection. It ultimately proves more powerful than a chemical or a nuclear weapon because it works silently and its effects can be far-reaching and uncontrollable. List of pathogenic bacteria that can be considered as possible biological warfare agents is unending [16]. Highly dangerous include *Botulinum toxin*, *Francisella tularensis*, *Salmonella typhimurium*, *Staphylococcus epidermis*, *Staphylococcus aureus* and *Yersinia pestis*. Other bio-agents, like *Venezuelan equine encephalitis*, *Marburg*, *Ebola*, and *influenza* viruses are of lesser importance, despite the fact, that infections with these viruses are serious and mortality is relatively high, but due to the difficulty in their preparation, their position on the list of Biological Warfare Agents (BWA) is lower. First evidence of bioterrorism came in to existence in 1979, when doctors presented a report of mass civilian death due to B. anthracis pneumonia i.e. due to inhalation of anthrax. A person exposed to B. Anthracis died immediately. The bacilli of anthracis multiply rapidly in the body and produce a harmful toxin that stops the process of breathing.

Different types of electrochemical biosensors which are in common practice are: Potentiometric, conductometric, amperometric, and impedimetric [17-20]. Out of these, amperometric biosensors are more common in practice and are usually based on ion-selective electrodes. These are three electrode based electrochemical systems which are attached with electrochemical detectors which measure the changes in ion concentration during reaction taking place in the bio-recognition layer. The advantage of Amperometric biosensors over other biosensors is that they are highly sensitive, rapid, linear concentration dependence and inexpensive [21]. Amperometric biosensors aimed at microbial analysis have been reported by different researchers [22-26].

In continuation to our earlier study [32], in this paper we have focussed on the fabrication of electrochemical biosensor for the detection of some pathogens as biological warfare agents.



II. MATERIALS AND METHOD

Samples of disease causing bacteria were collected from Microbial Type Culture Collection (MTCC), Institute of Microbial Technology, Chandigarh.

Different steps used for the electrochemical detection of disease causing bacteria are:

2.1 Preparation of Bacterial Strain

The bacterial test organism was grown in nutrient broth for 24 hours at 37.0 °C. A sodium phosphate buffer solution of pH 7.0 was prepared to hold these disease causing bacteria at a very low temperature i.e. 4.0 °C.

2.2 Synthesis of Metal Nanoparticles and Graphene:

Metalnanoparticles were synthesized by Co- precipitation technique. In this technique, solutions of different metal salts were reduced by using sodium hydroxide. Reduced graphene was synthesized by well known Hummers method.

2.3 Characterization of Metal Nanoparticles and Graphene

Characterization of Metal nanoparticles and graphene were carried out by using UV-visible spectroscopy, Fourier Transform Infra-Red (FT-IR) technique, X-ray diffraction (XRD) study and Transmission Electron Microscopy (TEM) techniques.

2.4 Fabrication of Working Test Electrode

A carbon paste (Graphene) working electrode was fabricated for the electrochemical determination of biological weapon. Slurry was prepared by mixing reduced graphene, alkaline phosphatase, cellulose acetate, Ferrocene, Horseradish peroxidase, aq. KOH and Poly (vinyl pyrolidone) (PVP). This slurry was filled in working test electrode with the help of luggin capillary. A copper wire was dipped from outside in the slurry for making electrical connections.

2.5 Fabrication of Three electrodes based Electrochemical Cell:

Three electrodes based electrochemical cell was fabricated having three electrodes i.e. a working test electrode (cellulose acetate, PVP bound carbon paste electrode), Ag/AgCl reference electrode and a platinum electrode acting as an auxiliary electrode for the electrochemical determination of disease causing pathogen (Figure 1).

2.6 Electrochemical Characterization

Three electrodes based electrochemical cell is connected to the instrument electrochemical workstation PGSTAT 128N, Metrohm Autolab attached to a PC and digital controlled water bath to maintain constant temperature. Electrochemical measurement experiments were performed on pathogenic bacteria and change in Open Circuit Potential (OCP), current (nA) and potential values were recorded at different conditions.



For the electrochemical characterization, 3×10^7 CFU of pathogen in 50.0 ml of PBS buffer solution was used. Four different samples were prepared i.e. pure PBS buffer solution as sample 1, PBS buffer solution with metal nanoparticles as sample 2, PBS buffer solution with 3×10^7 CFU of pathogen as sample 3, and PBS buffer solution with metal nanoparticles and 3×10^7 CFU of pathogen as sample 4.

The above samples were kept under following two observations:

- a) Heating at a constant temperature of 70.0 °C without stirring for 3.0 hours.
- b) Continuous stirring for 3.0 hours at room temperature.

After 3.0 hours, we have recorded the current and potential values and cyclic voltametry with the help of three electrodes based electrochemical cell connected to the instrument PGSTAT 128N, Metrohm Autolab, Netherland.

III. RESULTS

Figure 1 shows electrochemical biosensor for the detection of biological warfare agent. Figure 2 shows current and potential values of pure PBS buffer solution at 0.0 and after 3.0 hours of stirring at room temperature. Figure 3 shows current and potential behaviour of PBS buffer solution in presence of Metalnanoparticles (50.0 $\mu\text{l}/\text{ml}$) at 0.0 and after 3.0 hours of stirring at room temperature. Figure 4 shows current and potential behaviour of PBS buffer solution in presence of pathogen at 0.0 and after 3.0 hours of heating. Figure 5 shows current and potential behaviour of PBS buffer solution in presence of pathogen and Metalnanoparticles (50.0 $\mu\text{l}/\text{ml}$) at 0.0 and after 3.0 hours of stirring at room temperature.

Figure 6 shows chronoamperometry for pure PBS buffer solution at 0.0 and after 3.0 hours of stirring at room temperature. Figure 7 shows chronoamperometry for PBS buffer solution in presence of Metalnanoparticles (50.0 $\mu\text{l}/\text{ml}$) at 0.0 and after 3.0 hours of stirring at room temperature. Figure 8 shows Chronoamperometry for PBS buffer solution in presence of pathogen at 0.0 and after 3.0 hours of heating at 70.0⁰ C. Figure 9 shows chronoamperometry for PBS buffer solution in presence of pathogen and Metalnanoparticles (50.0 $\mu\text{l}/\text{ml}$) at 0.0 and after 3.0 hours of stirring at room temperature.

Figure 10 shows UV-visible spectra of Fe_3O_4 metal nanoparticles synthesized by co-precipitation technique. Figure 11 shows Fourier Transform Infra-Red (FT-IR) spectra (Thermo-USA, FTIR-3800) in the wavelength range of 400 - 4000 cm^{-1} of Fe_3O_4 metal nanoparticles synthesized by co-precipitation method. Figure 12 shows XRD pattern of Fe_3O_4 metal nanoparticles synthesized by co-precipitation method. Figure 13 shows TEM images of Fe_3O_4 metal nanoparticles synthesized by co-precipitation method.

IV. DISCUSSION

The UV absorption band of iron oxide nanoparticles (Figure 11) was observed in the wavelength range of 330–450.0 nm which may be due to the absorption and scattering of light by iron oxide nanoparticles [33-34]. The low absorption band at a wavelength of 410.0 nm may be due to the formation of least agglomerated Fe_3O_4



nanoparticles. Further, no additional peaks were observed corresponding to alcohol which indicates that the iron nanoparticles were not encapsulated by ethanol and they only acted as a soft template.

An absorption peak at $3,440\text{ cm}^{-1}$ in the FTIR spectrum of iron oxide nanoparticles (Figure 11), (characteristic peak of OH stretching vibration) confirms the presence of some amount of ferric hydroxide in Fe_3O_4 [35-36]. The other two distinct peaks at 565 and 421.0 cm^{-1} are due to the vibrations of $\text{Fe}^{2+}-\text{O}^{2-}$ and $\text{Fe}^{3+}-\text{O}^{2-}$ respectively [37]. Another peak (sharp and high intensity) at 565 cm^{-1} indicates the presence of high degree of crystallinity in the Fe_3O_4 nanoparticles. The characteristic absorption bands at 565 and 421 cm^{-1} confirms the presence of spinel structure in Fe_3O_4 nanoparticles. FT-IR spectroscopic technique was carried out in order to ascertain the purity and nature of ferrite metal nanoparticles synthesized by sol-gel technique.

The reflection peak at $2\theta = 35.60^\circ$ confirm spinel phase of ferrite (Fe_3O_4) nanoparticles (JCPDS, PDF cards 3-864 and 22-1086) (Figure 16). The diffractions peaks of the ferrite nanoparticles were observed at $2\theta = 30.18^\circ$ ($d = 0.297\text{ nm}$), 35.61° ($d = 0.253\text{ nm}$), 43.27° ($d = 0.209\text{ nm}$), 53.56° ($d = 0.171\text{ nm}$) and 57.11° ($d = 0.162\text{ nm}$) [23]. The peaks at an angle of 30.18° (220), 35.612° (311), 43.278° (400), 53.569° (422), 57.118° (511) and 62.655° (440) correspond to Fe_3O_4 . The average particle size of ferrite nanoparticles has been calculated using well known Scherrer equation [39] and was found to be 31.0 nm . Further, diffraction peak broadening confirms the formation of the ultrafine ferrite nanoparticles.

Structural and optical properties of Fe_3O_4 metal nanoparticles were determined by using Transmission Electron Microscope (TEM) of made Morgagni 268 D, FEI Philips at a resolution of 2 \AA from Electron Microscope Facility (SAIF), AIIMS, New Delhi (Figure 13). The TEM images reveals self-organized network like morphology of ferrite (Fe_3O_4) nanoparticles which are almost identical in shape and appear to be uniformly dispersed. The average particles size is in close agreement with both the technique i.e. as observed in TEM and the crystallite size calculated by the Scherrer equation ($\sim 31.0\text{ nm}$) with the help of XRD technique. Further, the TEM diffraction ring (Figure 17 b) confirms that the ferrite nanoparticles are in a well crystalline state [40].

It is also observed that open circuit potential (OCP) values of pathogen decreases on addition of metal nanoparticles which means that the metal nanoparticles are showing antibacterial properties and make the pathogen inactive. This may be due to the penetration of nanoparticles deep inside the bacteria through bacterial cell wall and thus making it inactive.

Heating of samples to 70.0°C leads to decrease in the OCP value from 0.240 to 0.185 V with $3.0 \times 10^7\text{ CFU}$ of pathogen and from 0.228 to 0.180 V with $3.0 \times 10^7\text{ CFU}$ of pathogen and Fe_3O_4 nanoparticles ($50\text{ }\mu\text{l/ml}$). Heating of samples to 70.0°C makes bacterial cell inactive just like addition of nanoparticles which lowers its OCP value.

Thus, it is concluded that heating of samples to 70.0°C for 3.0 hours and addition of metal nanoparticles ($50\text{ }\mu\text{l/ml}$) at room temperature have same effect i.e. both result in decrease in OCP value of PBS buffer solution

with 3.0×10^7 CFU of pathogen. Hence, it is concluded that an OCP value of phosphate buffer solution confirms the presence of pathogenic bacteria. Heating of the samples up to $70.0\text{ }^\circ\text{C}$ for a definite period of time leads to decrease in OCP value. Addition of metal nanoparticles also leads to decrease in OCP value i.e. heating and additions of metal nanoparticles have same effect on pathogen which lowers its OCP value.

V. CONCLUSION

A carbon (Graphene) based working electrode having alkaline phosphatase, cellulose acetate, Ferrocene, Horseradish peroxidase, aq. KOH and PVP was fabricated which when combined with Ag/AgCl reference and a platinum auxiliary electrode to form a three electrode based electrochemical cell for the electrochemical detection of pathogen as biological warfare agent. Metal nanoparticles were synthesized by co- precipitation method. Characterization of metal nanoparticles was carried out by using UV-visible, FT-IR, XRD and TEM techniques. An UV-visible absorption band at the wavelength of 410.0 nm and a sharp absorption band at 600.0 cm^{-1} in FTIR spectra confirm the formation of ferrite nanoparticles. Heating of samples to $70.0\text{ }^\circ\text{C}$ for 3.0 hours and addition of metal nanoparticles ($50.0\text{ }\mu\text{l/ml}$) at room temperature have same effect i.e. both results in decrease in OCP value. The values of both current and potential decrease on addition of metal nanoparticles ($50.0\text{ }\mu\text{l/ml}$). Continuous stirring of the samples of PBS and pathogen in presence of metal nanoparticles for a definite time leads to decrease in current value. This may be due to escaping of metal nanoparticles from bacterial cell thus making pathogen again in active form. A constant OCP value of 0.240 V in phosphate buffer solution indicates the presence of pathogenic bacteria in the sample.

VI. ACKNOWLEDGEMENT

We are very thankful to DRDO, New Delhi for providing us financial support for this research work.

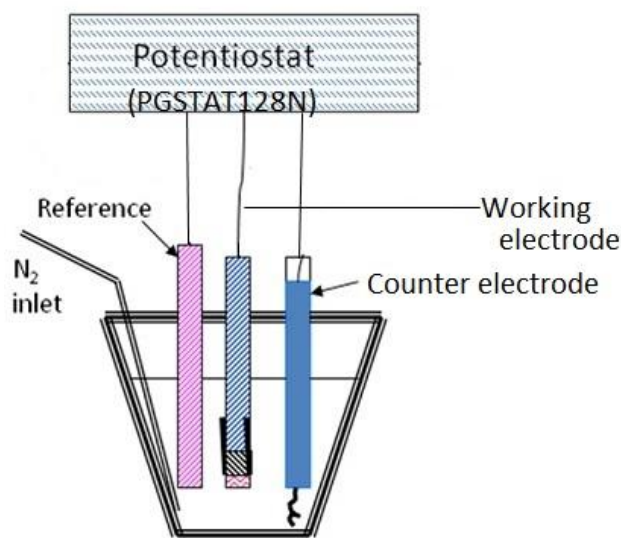


Fig.1. Electrochemical biosensor for the detection of biological warfare agent .

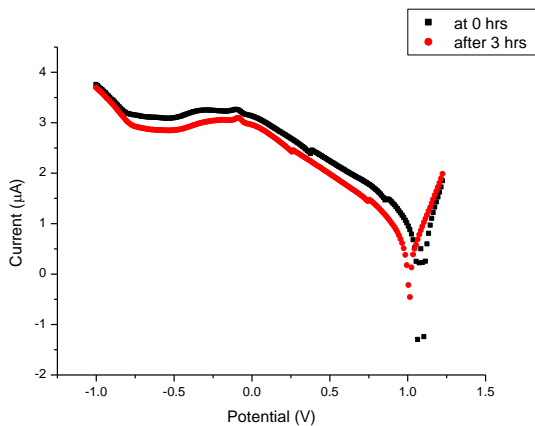


Fig. 2. Current vs potential behaviour of Pure PBS buffer solution at 0.0 and after 3.0 hours of stirring.

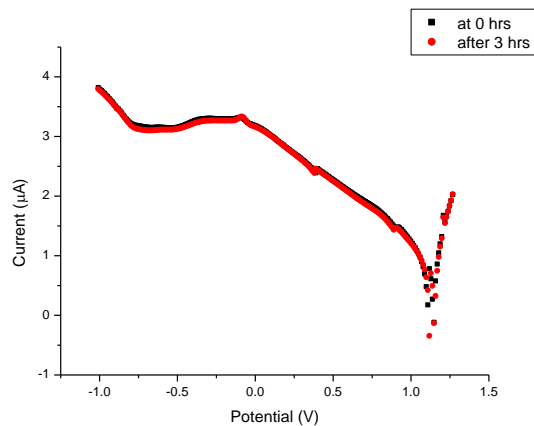


Fig. 3. Current vs potential behaviour of PBS buffer solution in presence of Fe₃O₄ nanoparticles (50.0 μl/ml) at 0.0 and after 3.0 hours of stirring.

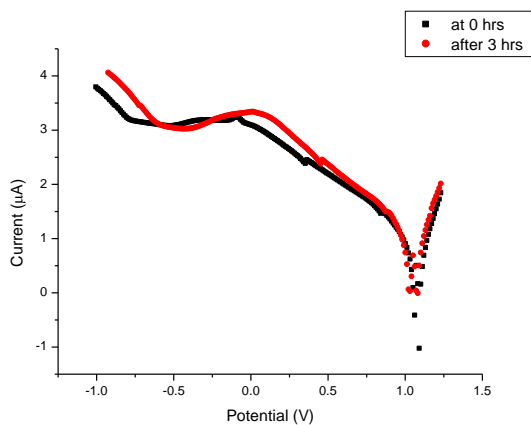


Fig. 4. Current vs potential behaviour of PBS Buffer solution with *S. aureus* at 0.0 and after 3.0 hours of heating.

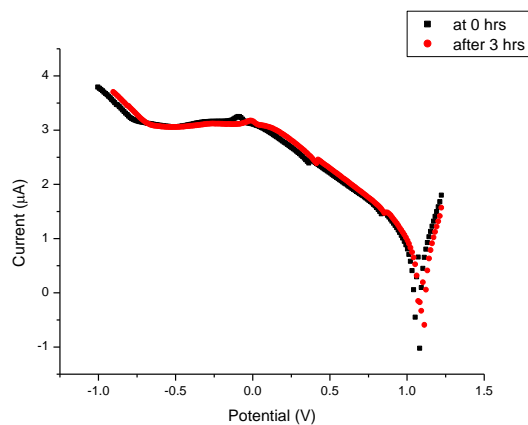


Fig. 5. Current vs potential behaviour of PBS buffer solution in presence of *S. aureus* and Fe₃O₄ nanoparticles (50.0 μl/ml) at 0.0 and after 3.0 hours of stirring.

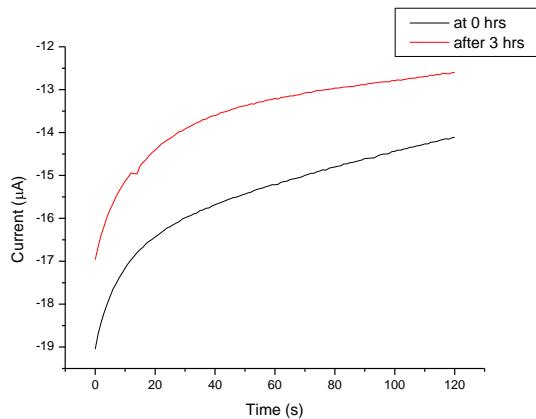


Fig. 6. Chronoamperometry for pure PBS buffer solution at 0.0 and after 3.0 hours of stirring.

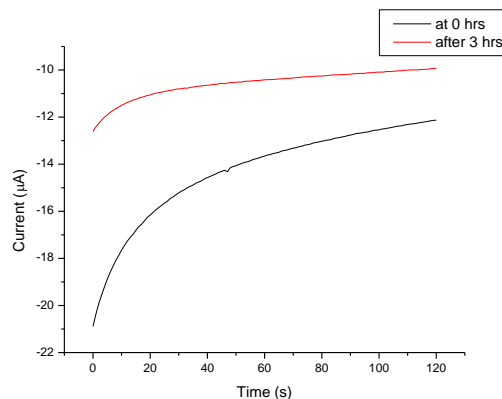


Fig. 7. Chronoamperometry for PBS buffer solution in presence of Fe₃O₄ nanoparticles (50.0 µl/ml) at 0.0 and after 3.0 hours of stirring.

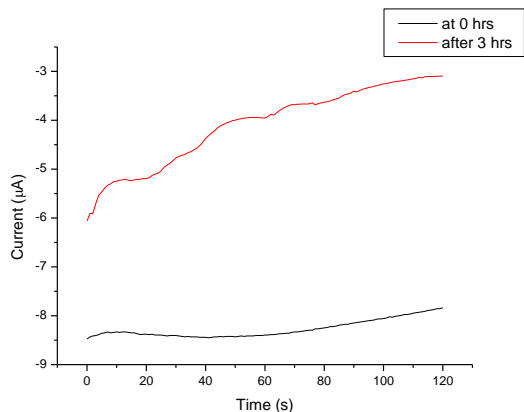


Fig. 8. Chronoamperometry for PBS buffer solution with *S. aureus* at 0.0 and after 3.0 hours of heating.

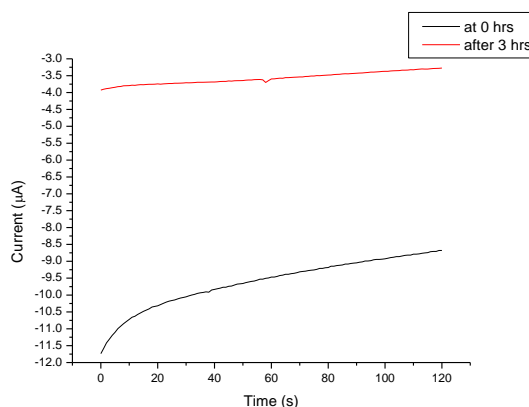


Fig. 9. Chronoamperometry for PBS buffer solution in presence of *S. aureus* and Fe₃O₄ nanoparticles (50.0 µl/ml) at 0.0 and after 3.0 hours of stirring.

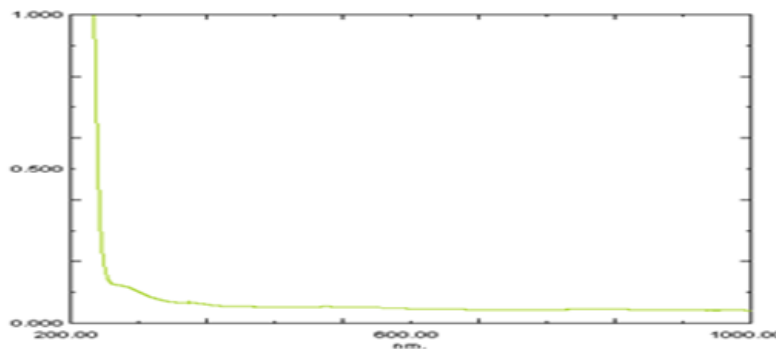


Fig. 10. UV-Visible spectra of Fe₃O₄ nanoparticles .

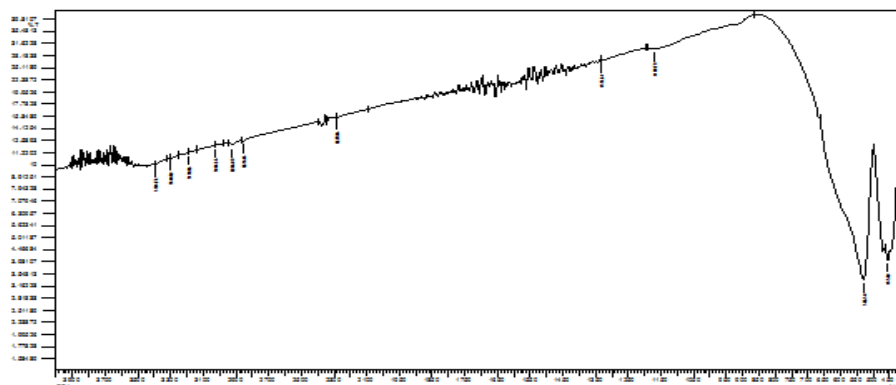


Fig.11. FT-IR spectra of Fe₃O₄ nanoparticles.

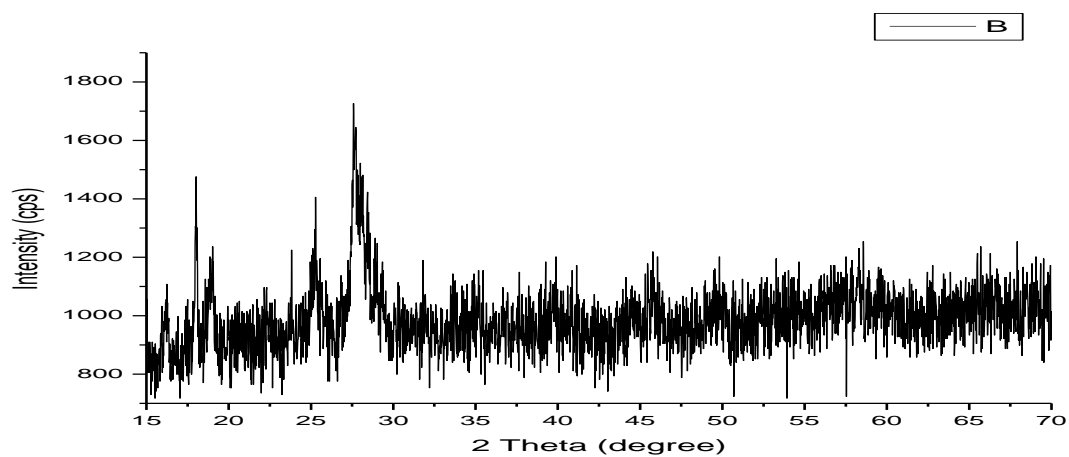


Fig. 12. XRD diffraction pattern of Fe₃O₄ nanoparticles.

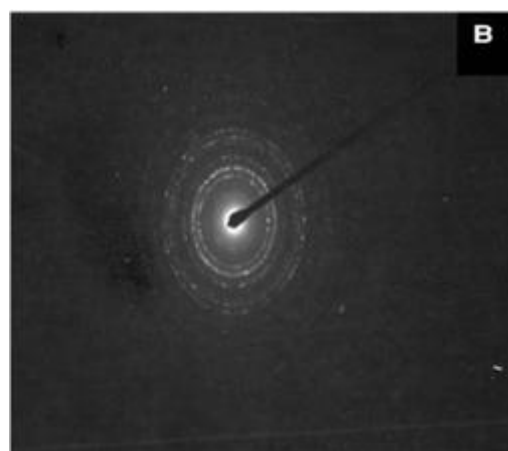
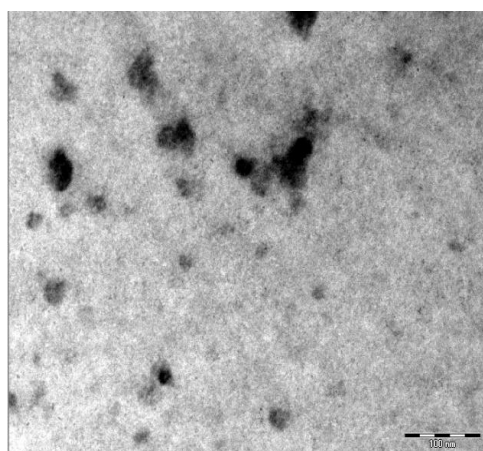


Figure13. (a) TEM images of Fe₃O₄ nanoparticles (b) Diffraction pattern of Fe₃O₄ nanoparticles.



REFERENCES

- [1] C. Buzea, I.I. Pacheco, K. Robbie, Nanomaterials and nanoparticles: Sources and toxicity, *Biointerphases* 2 (2007) Mr17–Mr71.
- [2] S.J. Klaine, P.J.J. Alvarez, G.E. Batley, T.F. Fernandes, R.D. Handy, D.Y. Lyon, S. Mahendra, M.J. McLaughlin, J.R. Lead, Nanomaterials in the environment: behavior, fate, bioavailability, and effects, *Environ. Toxicol. Chem.* 27 (2008) 1825–1851.
- [3] M. Farre, K. Gajda-Schrantz, L. Kantiani, D. Barcelo, Ecotoxicity and analysis of nanomaterials in the aquatic environment, *Anal. Bioanal. Chem.* 393 (2009) 81–95.
- [4] S. Sharifi, S. Behzadi, S. Laurent, M.L. Forrest, P. Stroeve, M. Mahmoudi, Toxicity of nanomaterials, *Chem. Soc. Rev.* 41 (2012) 2323–2343.
- [5] Geim, A.K., Novoselov, K.S., 2007. The rise of graphene. *Nat. Mater.* 6 (3), 183–191.
- [6] Wang, J., 2005. Carbon-nanotube based electrochemical biosensors: a review. *Electroanalysis* 17 (1), 7–14.
- [7] Shao, Y., Wang, J., Wu, H., Liu, J., Aksay, I.A., Lin, Y., 2010. Graphenebased electrochemical sensors and biosensors: a review. *Electroanalysis* 22 (10), 1027–1036.
- [8] Zhou, M., Zhai, Y., Dong, S., 2009b. Electrochemical sensing and biosensing platform based on chemically reduced graphene oxide. *Anal. Chem.* 81 (14), 5603–5613.
- [9] Clark Jr., L.C., Wolf, R., Granger, D., Taylor, Z., 1953. *J. Appl. Physiol.* 6(3), 189–193.
- [10] Lou, S.C., Patel, C., Ching, S.F., Gordon, J., 1993. *Clin. Chem.* 39(4), 619–624.
- [11] Cho, J.H., Paek, S.H., 2001. *Biotechnol. Bioeng.* 75(6), 725–732.
- [12] Lönnberg, M., Carlsson, J., 2001. *Anal. Biochem.* 293, 224–231.
- [13] Ho, J.A., Wauchope, R.D., 2002. *Anal. Chem.* 74, 1493–1496.
- [14] Shyu, R.H., Shyu, H.F., Liu, H.W., Tang, S.S., 2002. *Toxicol.* 40, 255–258.
- [15] Costa, M.N., Veigas, B., Jacob, J.M., Santos, D.S., Gomes, J., Baptista, P.V., Martins, R., Inácio, J., Fortunato, E., 2014. *Nanotechnology* 25, 1–12.
- [16] North Atlantic Treaty Organization. NATO Handbook on the Medical Aspects of NBC Defensive Operations, Part II, Biological NATO Amed. P-6(B) (1996).
- [17] I. Karube, K. Hara, H. Matsuoka, & S. Suzuki, (1982) Amperometric determination of total cholesterol in serum with use of immobilized cholesterol esterase and cholesterol oxidase. *Anal. Chim. Acta.*, 139, 127–32.
- [18] V. Veldhoven, P. P. Meyhi, & G. P. Mannaerts, (1998), Enzymatic quantization of cholesterol esters in lipid extracts. *Anal. Biochem.* 258, 152–55.
- [19] B. Shahnaz, S. Tada, T. Kajikawa, T. Ishida & K. Kawanishi, (1998) Automated fluorimetric determination of cellular cholesterol. *Ann. Clin. Biochem.* 345, 665–70.
- [20] J. F. Kennedy, A. In: Wiseman, (1975) (ed.) *Handbook of Enzyme Biotechnology*, Chap John Wiley and Sons, New York.
- [21] S. Singh, P. R. Solanki, & B. D. Malhotra, (2006) Covalent immobilization of cholesterol esterase and cholesterol oxidase on polyaniline films for application to cholesterol biosensor. *Anal. Chim. Acta.*, 568, 126–32.
- [22] J. F. Kennedy (1985) *Handbook of Enzyme Technology*, Marcel Dekker, New York.
- [23] W. E. Lee, H. G. Thomson, J. G. Hall, R. E. Fulton & J. P. Wong (1993) Characteristics of the Biochemical detector sensor. Defence Research Establishment Suffield, Canada. Suffield Memorandum No.1402, 1-23.



- [24] C. Ercole, M. Del Gallo, M. Pantalone, S. Santucci, L. Mosiello, C. Laconi & Lepidi. (2002) Sensor Actuators B, 4163, 1-5.
- [25] A. L. Ghindilis, P. Atanasov, P. Wilkins & E. Wilkins. (1998) A biosensor for Escherichia coli based on a potentiometric alternating biosensing (PAB) transducer. Biosensors Bioelectronics, 13, 113-31.
- [26] E. L. Crowley, C. K. O'Sullivan & G. G. Guilbault. (1999) Increasing the sensitivity of listeria monocytogenes assays: evaluating using ELISA and amperometric detection. Analyst, 124(3), 295-99.
- [27] B. Mirhabibollahi, J. L. Brooks & R. G. Kroll. (1990) A semi-homogeneous amperometric immunosensor for protein A-bearing Staphylococcus aureus in foods. Appl. Microbiol. Biotechnol. 34, 242.
- [28] J. L. Brooks, B. Mirhabibollahi & R. G. Kroll. (1990) Sensitive enzyme-amplified electrical immunoassay for protein A-bearing S. Aureus in food. Appl. Environ. Microbiol. 56, 3278-84.
- [29] N. Nakamura, A. Shigematsu & T. Matsunaga. (1991) Electrochemical detection of viable bacteria in urine and antibiotic selection. Biosens. Bioelectron. 6, 575.
- [30] J. L. Brook, B. Mirhabibollahi & R. G. Kroll. (1992) Experimental enzyme linked immunosensor for the detection of Salmonella in food. J. Appl. Bacteriology. 73, 189-96.
- [31] H. J. Kim, H. P. Bennetto & M. A. Haqlablab. (1995) A novel liposome based electrochemical biosensor for the detection of haemolytic microorganisms. Biotechnol. Tech., 9(6), 389-94.
- [32] H. Kumar & R. Rani. (2013) Development of Biosensor for the detection of Biological Warfare Agents: Its Issues & Challenges. Sci. Progress, 96(3), 294-308.
- [33] T. Koutzarova, S. Kolev, C. Ghelev, D. Paneva & I. Nedkov. (2006) Microstructural study and size control of iron oxide nanoparticles produced by microemulsion technique. Phys. Stat. Sol.(c). 3(5), 1302-07.
- [34] X. J. Bard & L. R. Faulkner. (2000) Electrochemical Methods: Fundamentals and Applications, 2nd edn, Wiley, New York.
- [35] X. Chen, Y. Wang, J. Zhou, W. Yan, X. Li & J. J. Hu. (2008) Electrochemical impedance immunosensor based on three-dimensionally ordered macroporous gold film. Anal. Chem. 80, 2133-40.
- [36] J. H. Meng, G. Q. Yang, L. M. Yan & X. Y. Wang. (2005) Synthesis and characterization of magnetic nanometer pigment Fe₃O₄. Dye. Pigments. 66, 109-13.
- [37] A. Kaushik, R. Khan, P. R. Solanki, P. Pandey, J. Alam, S. Ahmad & B. D. Malhotra. (2008) Iron oxide nanoparticles-chitosan composite based glucose biosensor. Biosens. Bioelectron. 24(4), 676-83.
- [38] R. Boistelle & J. P. Astier. (1988) Crystallization mechanism in solutions. J. Cryst. Growth. 90, 14-30.
- [39] H. K. Moudgil, (2015) A textbook of Physical Chemistry, 2nd Edn., Prentice Hall of India, Pvt. Ltd., New Delhi, 648-50.
- [40] J. Wang, Q. Chen, C. Zheng & B. Hou. (2004) Magnetic-field-induced growth of single-crystalline Fe₃O₄ nanowires. Adv. Mater. 16(2), 137-40.